<040121> Chem. Rev. 1994, 94, 2483–2547 Literature Seminor B4 Kazuki Sasaki

Catalytic Asymmetric Dihydroxylation

Contents
I) Introduction
II) Ligand Structure
III) Controversy over Mechanism

Hartmuth C. Kolb,† Michael S. VanNieuwenhze,‡ and K. Barry Sharpless*

Department of Chemistry, The Scripps Research Institute, 10666 North Torrey Pines Road, La Jolla, California 92037

Received July 28, 1994 (Revised Manuscript Received September 14, 1994)

I) Introduction

Scheme 1. The Osmylation of Olefins

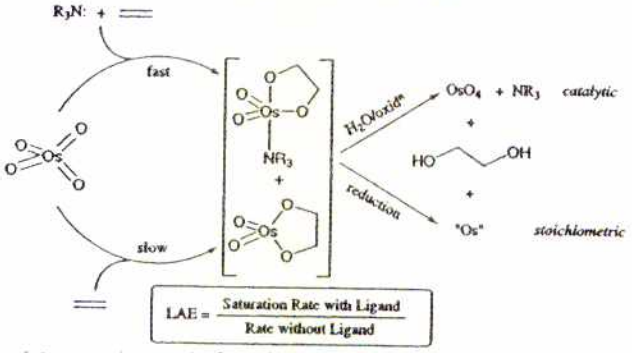

<Some ligand for AD>

(a) Cinchona Alkaloid Ligands for AD under *Catalytic* Conditions[16a,18,20,23]

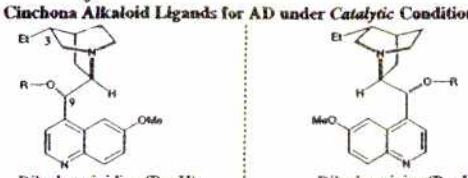

Dihydroquinidine (R = H) DHQD

Dihydroquinine (R = H) DHQ

(b) Recent Monodentate Ligands for AD under *Catalytic* Conditions

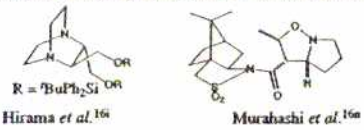

R = ^{t}BuPh$_2$Si

Hirama *et al.*[16i] Murahashi *et al.*[16n]

Second Generation Ligands

Phthalazine (PHAL) Ligands[23] (1)

Diphenylpyrimidine (PYR) Ligands[24] (2)

First Generation Ligands

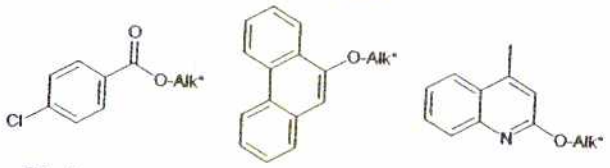

Chlorobenzoate (CLB) Ligands (3)

Phenanthryl Ether (PHN) Ligands[25] (4)

4-Methyl-2-quinolyl Ether (MEQ) Ligands[25] (5)

<Reaction Mechanism>

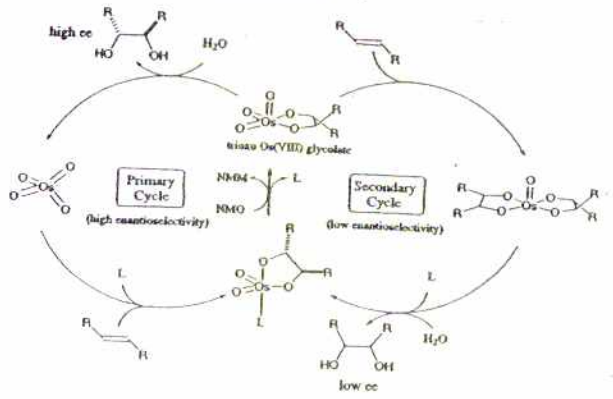

Table I. Enantiomeric Excesses Obtained in the Asymmetric Dihydroxylation of Olefins under Different Conditions

			catalytic	
entry	olefin	stoichiometric[a]	original[b]	slow addition[d]
1		61	56	60 (5 h)
2	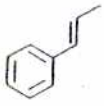	87	65	86 (5 h)
3	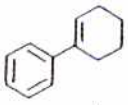	79	8[c]	78 (26 h)[f]
4	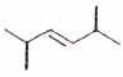	80	12[g]	46 (24 h)[h]
5		69	20	70 (10 h)

Scheme 3. Catalytic Cycle of the AD Reaction with $K_3Fe(CN)_6$ as the Cooxidant[20]

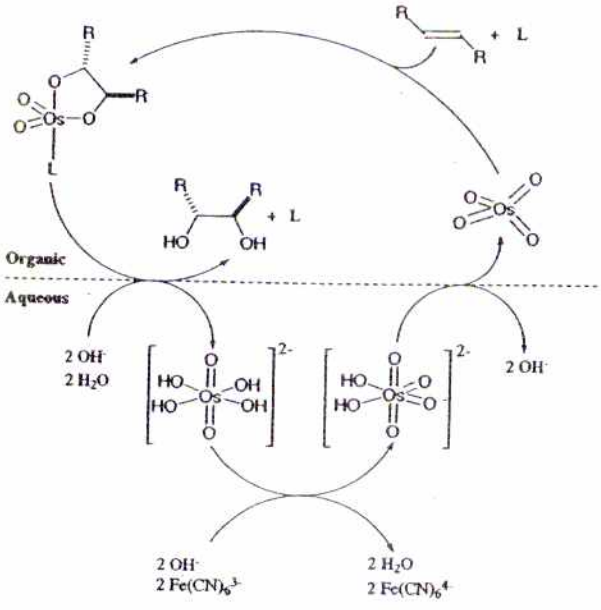

Scheme 4. Schematic Presentation of the Concerted [3 + 2] Mechanism[9e] (Path A) and the Stepwise Osmaoxetane Mechanism[9f,g] (Path B)

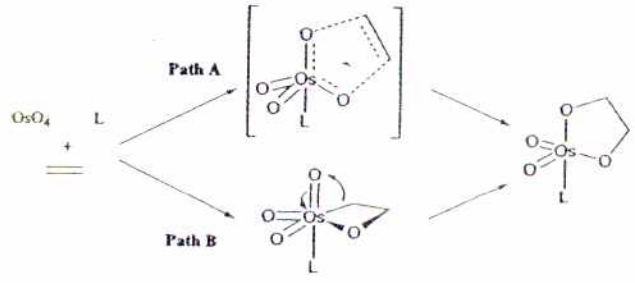

II) Ligand Structure

J. Am. Chem. Soc. 1994, *116*, 1278–1291

Toward an Understanding of the High Enantioselectivity in the Osmium-Catalyzed Asymmetric Dihydroxylation (AD). 1. Kinetics

Hartmuth C. Kolb, Pher G. Andersson, and K. Barry Sharpless*

Contribution from the Department of Chemistry, The Scripps Research Institute, 10666 North Torrey Pines Road, La Jolla, California 92037

*Received October 12, 1993**

Chart 1. Saturation Plot Obtained with DHQD 9-*O*-*p*-chlorobenzoate (5) and Cyclohexene (*t*-BuOH, 25 °C, 680 nm, c_{OsO_4} = 0.000 12 mol/L, $c_{cyclohexene}$ = 0.011 mol/L)

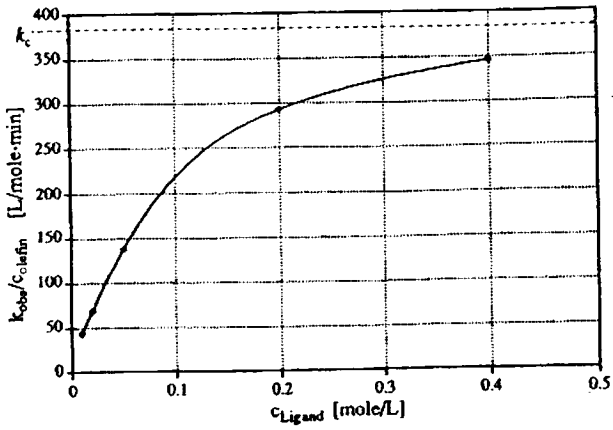

Scheme 4[a]

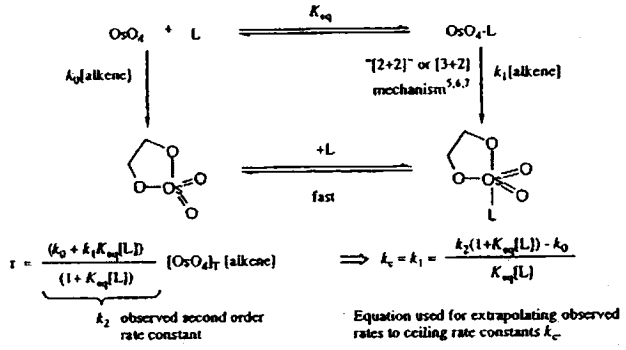

[a] $[OsO_4]_T$ is the total concentration of OsO_4 in the reaction mixture, defined as $[OsO_4]_T = [OsO_4] + [OsO_4{\cdot}L]$, and is independent of the ligand concentration.

- All rate measurements were carried out under stoichiometric conditions.
- k_c means saturation rate constant
- $r = \dfrac{k_0 + k_1 K_{eq}[L]}{1 + K_{eq}[L]} [OsO_4]_T [alkene]$

∵ $[OsO_4 \cdot L] = K_{eq}[OsO_4][L]$

$[OsO_4]_T = [OsO_4] + [OsO_4 \cdot L] = (1 + K_{eq}[L])[OsO_4]$

$r = k_1[OsO_4 L][alkene] + k_0[OsO_4][alkene]$

$= (k_1 K_{eq}[L] + k_0)[OsO_4][alkene]$

$= \dfrac{k_0 + k_1 K_{eq}[L]}{1 + K_{eq}[L]} [OsO_4]_T [alkene]$ //

- When the ligand acceleration effect (LAE) completely saturates, $k_1 K_{eq}[L] \gg k_0$ and $K_{eq}[L] \gg 1$.

At saturation, rate constant k_2 is k_c. ($= k_1$)

Chart 3. Saturation Rate Constants in Toluene at 25 °C

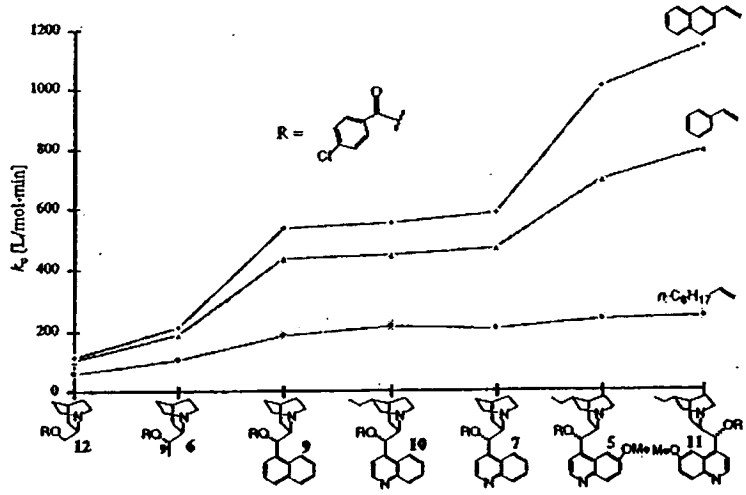

Chart 4. Saturation Rate Constants in *t*-BuOH at 25 °C

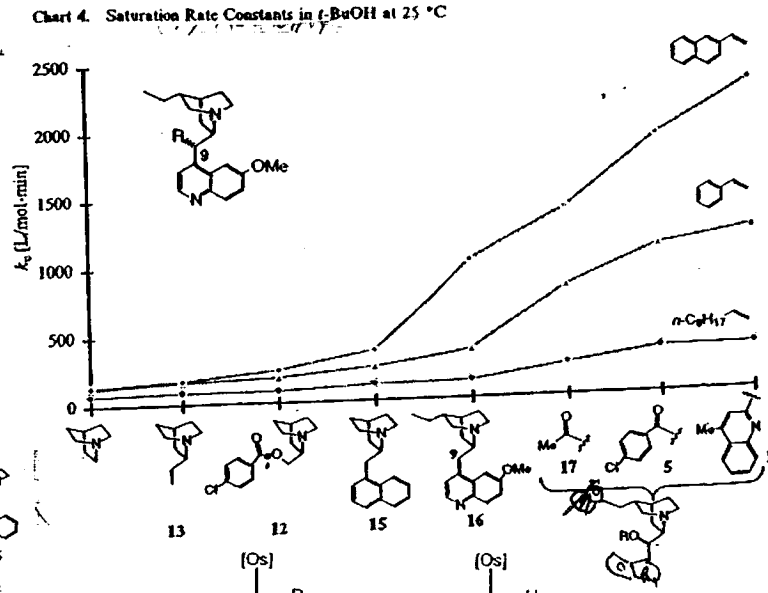

Chart 2. Binding Constants in Toluene.

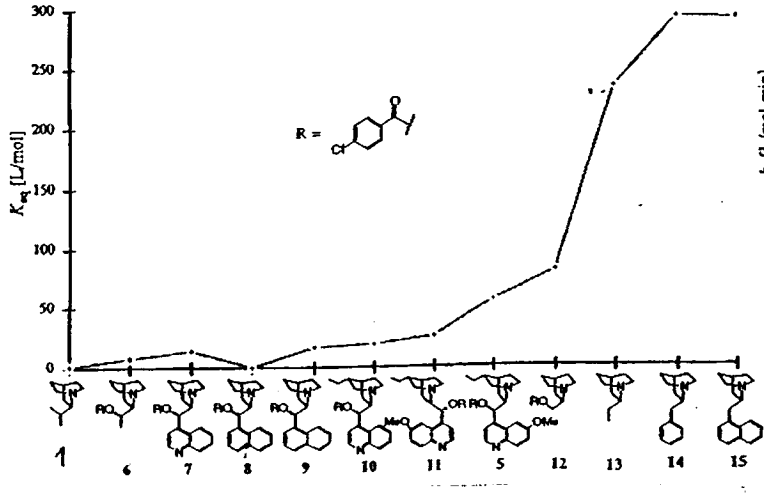

theo : 6
erythro : 7, 9, 10, 11, 5
DHQD : 5
DHQ : 11

Keq : 60000 [L/mol]
(quinuclidine)

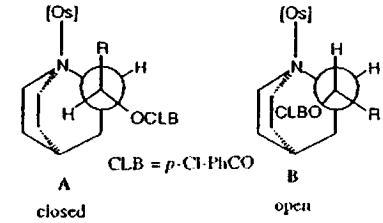

Figure 2. Conformational analysis of the OsO_4 complexes of *erythro* cinchona analogs.[16]

②

Chart 5. Saturation Rate Constants for Dihydroquinidine Derivatives in *t*-BuOH at 25 °C

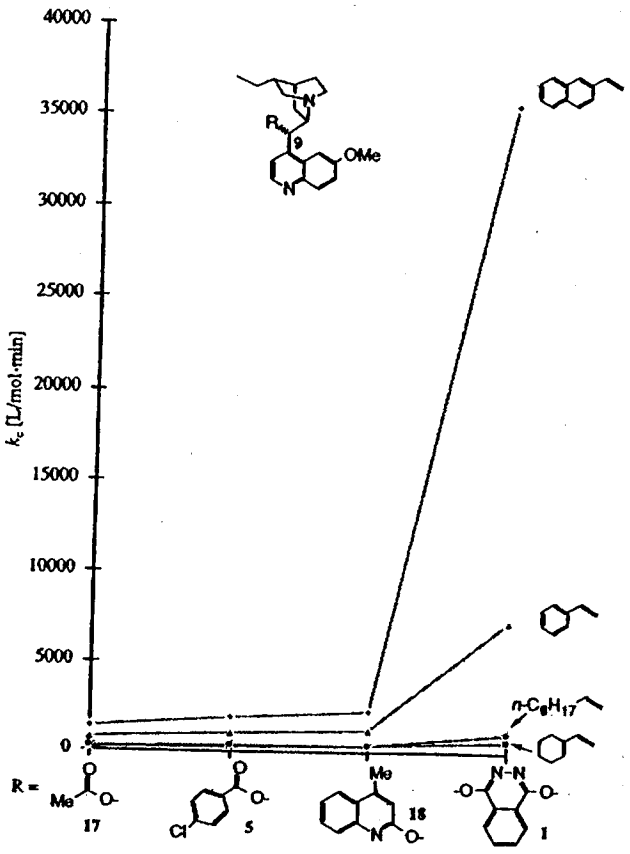

Table 1. Relationship between Enantioselectivities[1] and Ceiling Rate Constants[a]

	n-C_8H_{17} %ee	n-C_8H_{17} k_c	%ee	k_c	%ee	k_c
5	45[c]	331	74[b] 73[c]	1089	88[c]	1907
18	65[b]	335	87[b]	1210	93[b]	2287
1	84[b]	1065	97[b] 94[c,d]	7320	98[c,d]	35600

[a] Ceiling rate constants k_c [L/(mol·min)] were measured in *t*-BuOH at 25 °C by monitoring the appearance of the glycolate complex at 680 nm in a stopped-flow apparatus; all AD reactions were performed under catalytic conditions in 1:1 *t*-BuOH/H_2O, using $K_3Fe(CN)_6$ as the stoichiometric reoxidant (ref 1). [b] The AD reaction was performed at 0 °C. [c] The AD was carried out at room temperature. [d] Hartung, J.; Sharpless, K. B. Unpublished results.

Chart 6. Saturation Rate Constants versus Binding Constants in *t*-BuOH at 25 °C, Excluding $(DHQD)_2PHAL$ (1) and Quinuclidine, Which Are 'Off-Scale' [1: K_{eq} = 27.7 L/mol, k_c(2-vinylnaphthalene) = 35 600 L/(mol·min). Quinuclidine: K_{eq} = 2630 L/mol, k_c(vinylnaphthalene) = 147 L/(mol·min)]

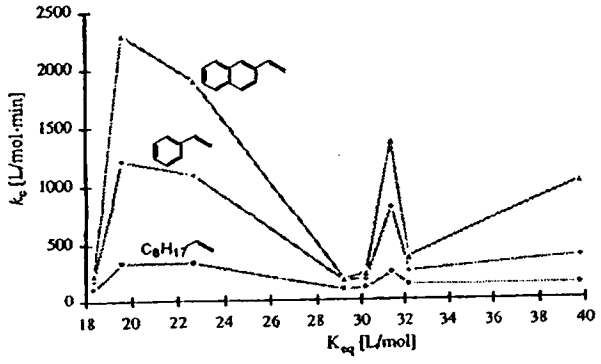

Chart 7. Effect of the Solvent on the Relative Rate Constants

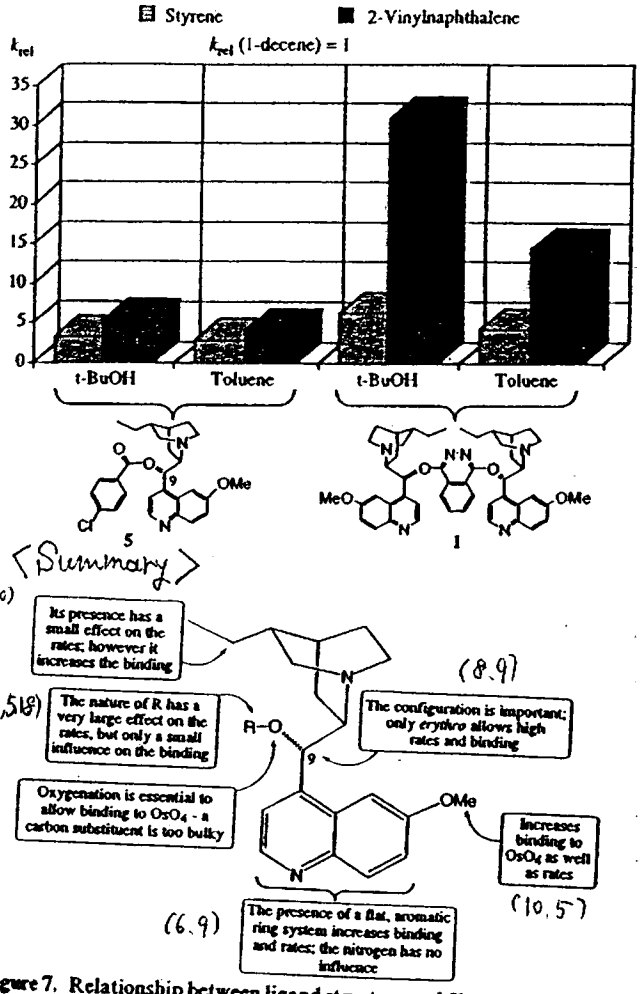

Figure 7. Relationship between ligand structure and K_{eq} and ceiling rate constants. The alkaloid core is ideally set up to ensure high rates, binding, and solubility. The rates are influenced considerably by the nature of the O9 substituent, while the binding to OsO_4 is almost independent of that substituent.

III) Controversy over Mechanism

[2+2] L-shape

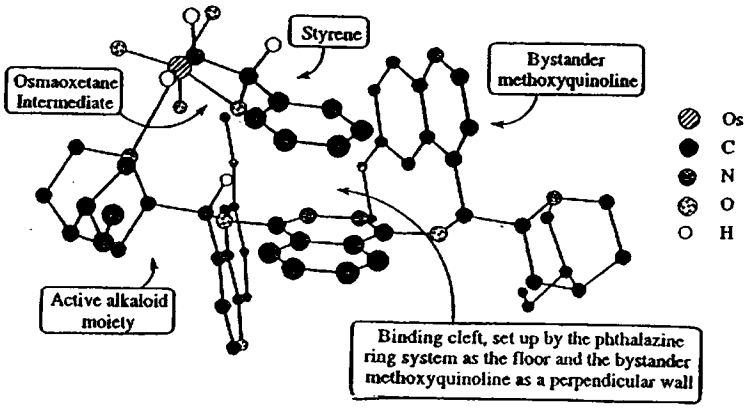

[3+2] U-shape

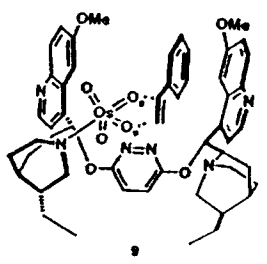

Ⅲ)-1 Origin of [2+2]

Chromyl Chloride Oxidations of Olefins. Possible Role of Organometallic Intermediates in the Oxidations of Olefins by Oxo Transition Metal Species

K. Barry Sharpless,* Alan Y. Teranishi, and Jan-E. Bäckvall

Contribution from the Department of Chemistry, Massachusetts Institute of Technology, Cambridge, Massachusetts 02139. *Received November 19, 1976*

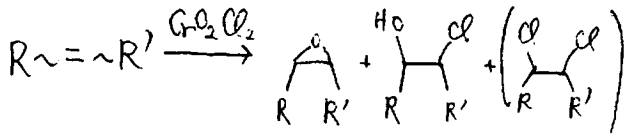

Table I. CrO_2Cl_2 Oxidations of Disubstituted Olefins[a]

Olefin	Epoxide Z	Epoxide E	Halohydrin Erythro	Halohydrin Threo	Halo ketone
1. (*E*)-Cyclododecene	2	20	5	60	8
2. (*Z*)-Cyclododecene	28	2	25	4	5
3. (*E*)-5-Decene	1	15	5	55	7
4. (*Z*)-5-Decene	13	2	35	30	5
5. (*Z*)-5-Decene[b]	0	0	28[c]	5[c]	35[d]
6. Cyclohexene	5		15	25	5

[a] Unless otherwise noted, all reactions were performed in CH_2Cl_2 at −78 °C using 1.3 equiv of CrO_2Cl_2. After 3 h the reaction mixture was poured into aqueous sodium sulfite at 0 °C. All yields were determined by GLC relative to an internal standard. [b] In this case the oxidation was run in acetone at −78 °C in the presence of excess LiBr. [c] Bromohydrins. [d] Bromo ketone.

Scheme III. Mechanism Involving Organometallic Intermediates

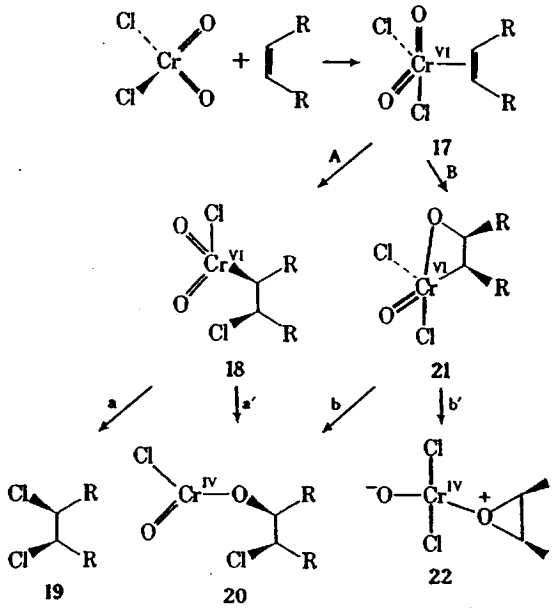

Scheme V

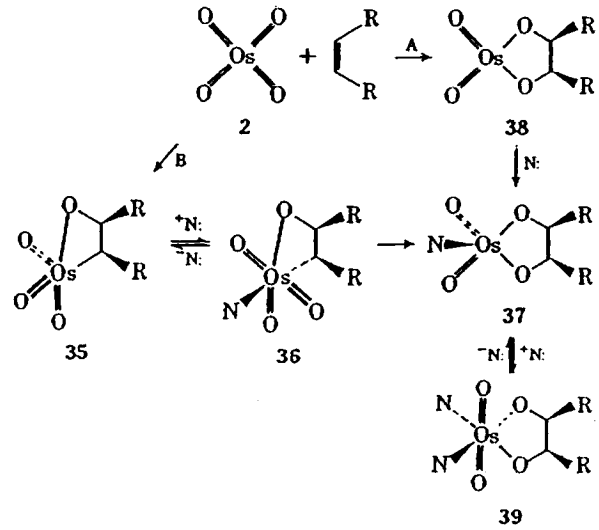

Ⅲ)-2 Support for [2+2]

Temperature Effects in Asymmetric Dihydroxylation: Evidence for a Stepwise Mechanism**

By *Thomas Göbel* and *K. Barry Sharpless**

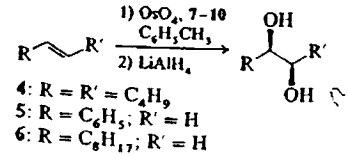

4: R = R′ = C_4H_9
5: R = C_6H_5; R′ = H
6: R = C_8H_{17}; R′ = H

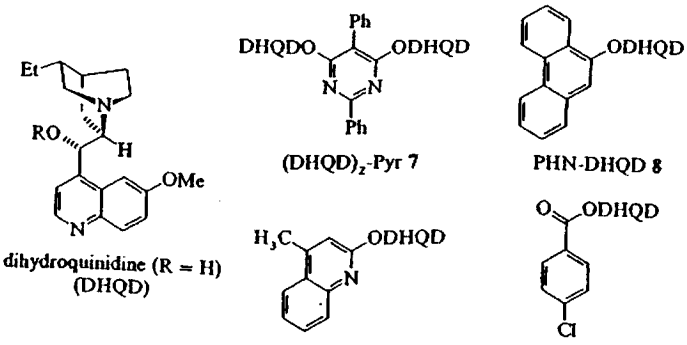

dihydroquinidine (R = H) (DHQD)

(DHQD)$_2$-Pyr 7

PHN-DHQD 8

MEQ-DHQD 9

CLB-DHQD 10

Scheme 3.

$$\ln \frac{k_{(major)}}{k'_{(minor)}} = -\frac{\Delta\Delta H^{\ddagger}}{RT} + \frac{\Delta\Delta S^{\ddagger}}{R}$$ (Eyring formalism)

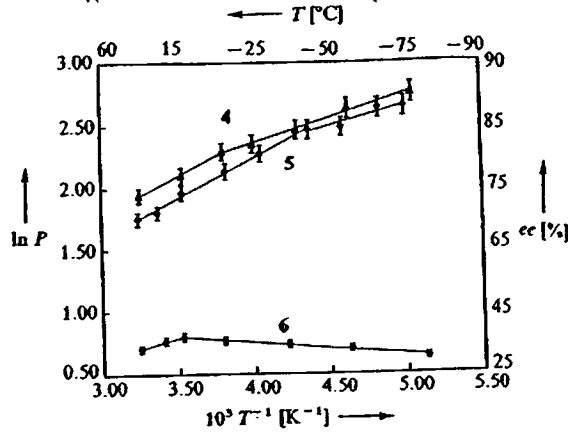

Fig. 1. Eyring plots for the enantiomeric excesses of the dihydroxylation of olefins 4–6 with 9 as ligand. The error bars represent confidence levels of ±95% and were determined by standard statistical analysis.

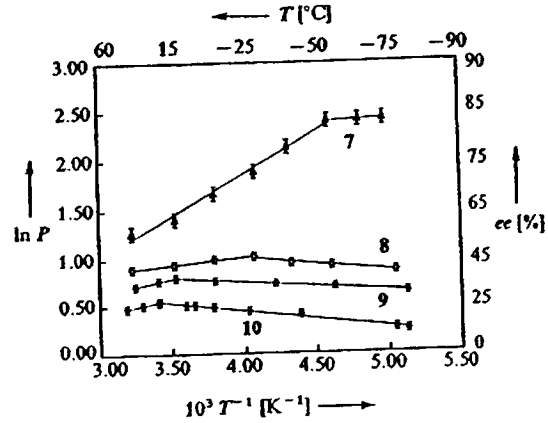

Fig. 2. Eyring plots for the enantiomeric excesses of the dihydroxylation of 1-decene (6) with the chiral alkaloid ligands 7–10. The error bars represent confidence levels of ±95% and were determined by standard statistical analysis.

* Inversion point existed. → $\Delta\Delta H^{\ddagger}$, $\Delta\Delta S^{\ddagger}$ aren't constant.
→ There should be at least two enantioselective steps.

J. Am. Chem. Soc. 1996, 118, 319–329 III)-3 Excuse against Eyling plot

Kinetic Investigations Provide Additional Evidence That an Enzyme-like Binding Pocket Is Crucial for High Enantioselectivity in the Bis-Cinchona Alkaloid Catalyzed Asymmetric Dihydroxylation of Olefins

E. J. Corey* and Mark C. Noe

Contribution from the Department of Chemistry, Harvard University, Cambridge, Massachusetts 02138

Received July 31, 1995®

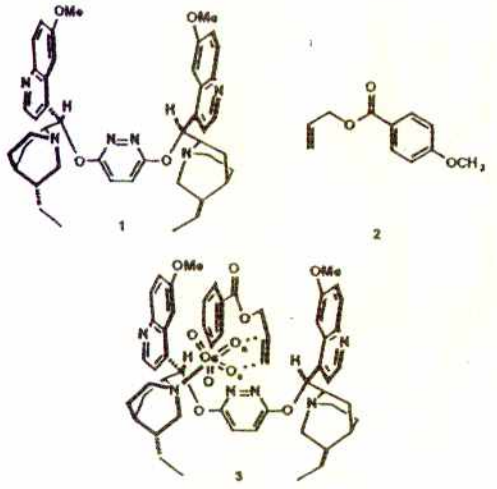

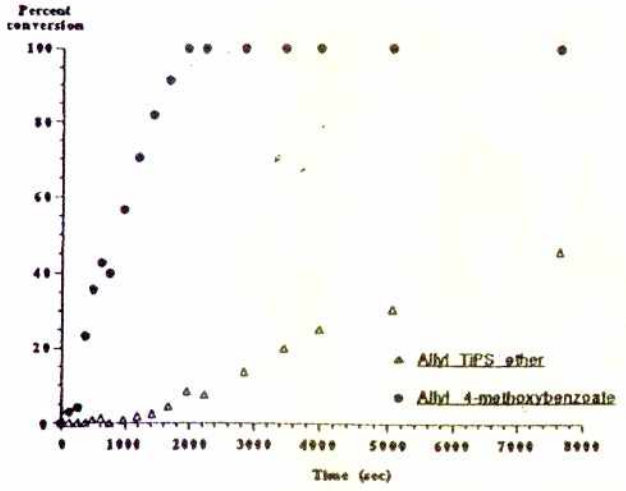

igure 3. Reaction profile for the competitive catalytic asymmetric hydroxylation of allyl 4-methoxybenzoate (2) (0.08 M) and allyl iisopropylsilyl ether (6) (0.08 M) using the $(DHQD)_2PYDZ$ ligand 1 6 mM) and $K_2OsO_4 \cdot 2H_2O$ (0.4 mM) in 1:1 *tert*-butyl alcohol–H_2O °C.

$$V = \frac{V_{max}[S]}{K_M + [S]}$$ (Michaelis-Menten)

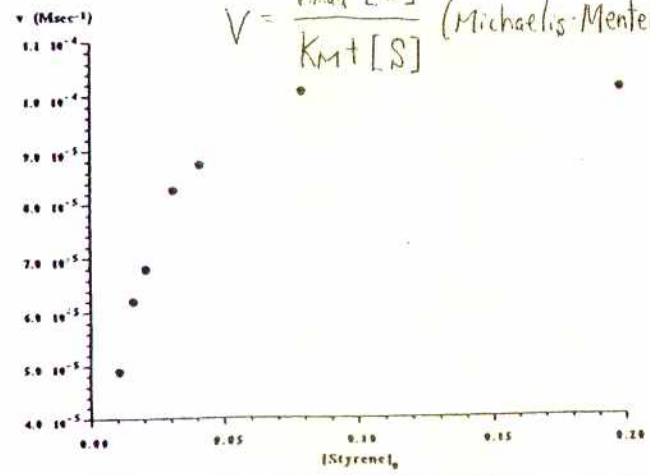

Figure 7. Plot of initial velocity versus initial olefin concentration showing saturation behavior for the $(DHQD)_2PYDZ \cdot OsO_4$ catalyzed asymmetric dihydroxylation using 1 mM $(DHQD)_2PYDZ$ ligand, 0.5 mM $K_2OsO_4 \cdot 2H_2O$ in 1:1 *tert*-butyl alcohol–water at 0 °C.

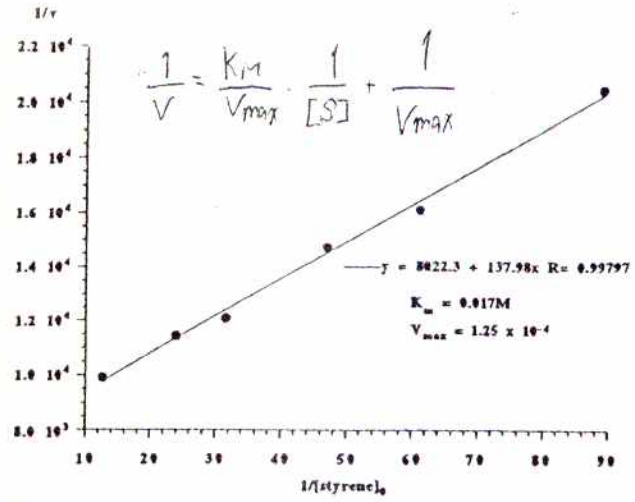

$$\frac{1}{V} = \frac{K_M}{V_{max}} \cdot \frac{1}{[S]} + \frac{1}{V_{max}}$$

Figure 8. Lineweaver–Burk plot for the catalytic asymmetric dihydroxylation of styrene under the conditions noted in Figure 7.

Table 1. Comparison of the Michaelis–Menten parameters K_m and V_{max} and Observed Enantioselectivity in the Catalytic Asymmetric Dihydroxylation of Olefins[a]

Entry	Olefin (formula no.)	K_m	V_{max}	% ee
1	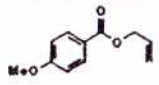 (2)	0.017M	1.1×10^{-4}	96[b,c]
2	 (6)	0.49M	5.5×10^{-6}	13[b,c]
3	 (7)	0.017M	1.3×10^{-4}	86[b,c,d]
4	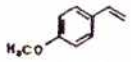 (8)	0.0068M	6.5×10^{-5}[f]	97[e]
5	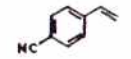 (9)	0.0068M	1.0×10^{-4}	97[e]
6	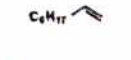 (10)	0.061M	3.8×10^{-5}	79[b,c,d]
7	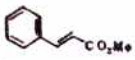 (11)	0.0075M	1.7×10^{-4}	96[e]
8	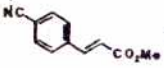 (12)	0.0045M	1.4×10^{-4}	96[e]
9	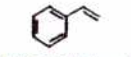 (7)	0.15M	4.0×10^{-5}	40[b,c]

DHQD-PYDZ-OMe Ligand (13)

[f] This reaction was performed using 0.5 mM $(DHQD)_2PYDZ$ ligand and 0.25 mM $K_2OsO_4 \cdot 2H_2O$

[e] This work.

[a] Unless otherwise indicated, all reactions were performed at 0 °C in 1:1 *tert*-butyl alcohol–water using the $(DHQD)_2PYDZ$ ligand (1 mM) and $K_2OsO_4 \cdot 2H_2O$ (0.5 mM).

Table 2. Observed and Calculated Initial Velocity Ratios (Φ) for Multiple Substrate Competition Experiments[a]

substrate combination	calcd Φ	obsd Φ
styrene–decene	12.3	8.6
decene–allyl TiPS ether	5.5	5.6
4-vinylanisole–styrene	5.0	4.2
4-vinylanisole–4-CN styrene	3.4	3.4

[a] All reactions were run with 0.04 M initial substrate concentration using 1 mM $(DHQD)_2PYDZ$ ligand and 0.5 mM $K_2OsO_4 \cdot 2H_2O$ at 0 °C in 1:1 *tert*-butyl alcohol–water. The faster reacting olefin is indicated first.

Table 3. Inhibition of the Catalytic Asymmetric Dihydroxylation of Styrene Using the $(DHQD)_2PYDZ{\cdot}OsO_4$ Catalyst $1{\cdot}OsO_4$

Inhibitor	K_i	Inhibitor	K_i
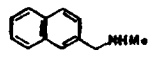 14	1.6 mM	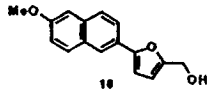 18	6.0 mM
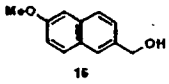 15	27 mM	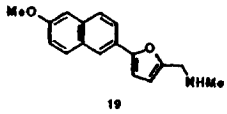 19	0.30 mM
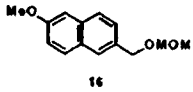 16	71 mM		
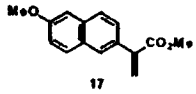 17	1.2 mM	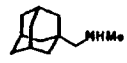 20	26 mM

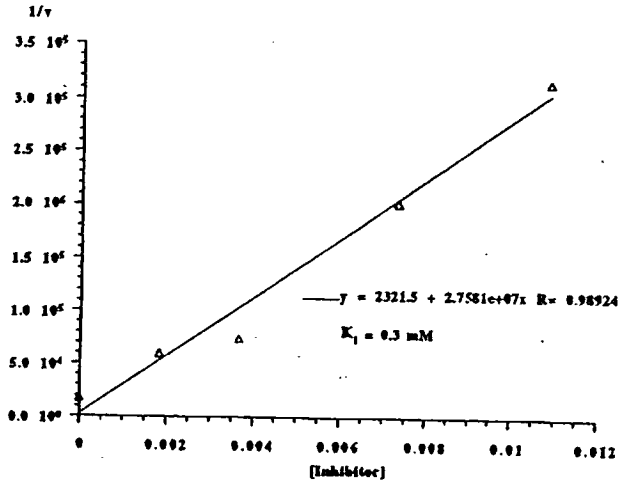

Figure 9. Dixon plot for the inhibition of the asymmetric dihydroxylation of styrene using the $(DQHD)_2PYDZ{\cdot}OsO_4$ catalyst by **19**. The initial styrene concentration was 17.5 mM. The reaction conditions are the same as those detailed in Figure 7.

* Kinetic studies on AD demonstrated Michaelis-Menten behavior. It means prior to transition state a rapidly and reversibly complex is formed.

→ Corey et al. revised [3+2] mechanism.

Scheme 1. Proposed CCN Pathway for the Production of the Osmium(VI) Ester of Styrene from Styrene and $1{\cdot}OsO_4$.

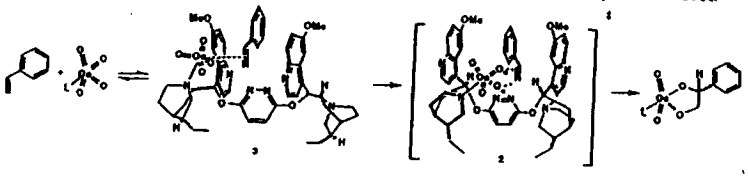

III)-4 Criticism against [2+2]

A Critical Analysis of the Mechanistic Basis of Enantioselectivity in the Bis-Cinchona Alkaloid Catalyzed Dihydroxylation of Olefins

E. J. Corey* and Mark C. Noe

Contribution from the Department of Chemistry, Harvard University, Cambridge, Massachusetts 02138

Received April 15, 1996®

[3+2]

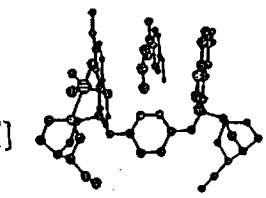

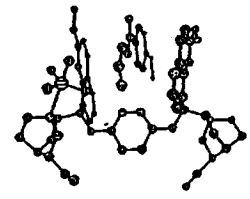

[2+2]

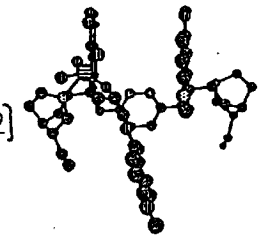

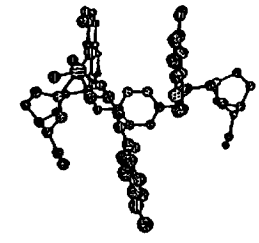

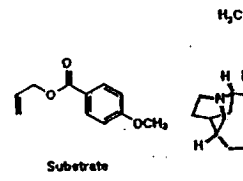

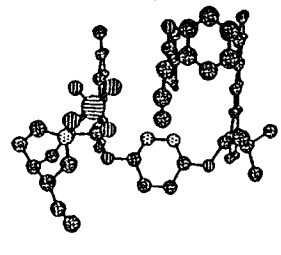

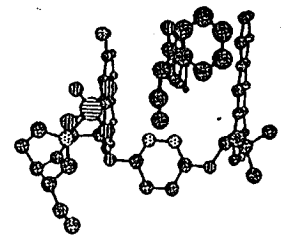

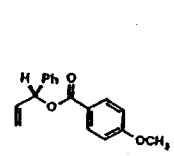

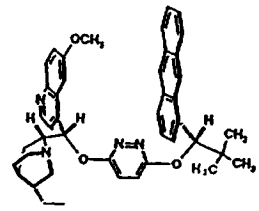

Table 7. Kinetic Resolution of Racemic Allylic 4-Methoxybenzoates Using Cinchona Alkaloid Ligands

Substrate	Ligand	k_{rel}[a]
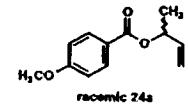 racemic 24a	$(DHQD)_2PYDZ$ (1)	3.1
	DHQD-PYDZ-(S)-anthryl (23)	20
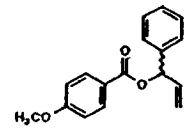 racemic 24b	$(DHQD)_2PYDZ$ (1)	1.9
	DHQD-PYDZ-(S)-anthryl (23)	79

[a] Relative rates of reaction of ent-**24** and **24**.

J. Am. Chem. Soc. 1997, 119, 1840–1858 III)-5 Search for the new mechanism.

Toward an Understanding of the High Enantioselectivity in the Osmium-Catalyzed Asymmetric Dihydroxylation. 4. Electronic Effects in Amine-Accelerated Osmylations

Derek W. Nelson,[†] Andreas Gypser,[†] Pui Tong Ho,[†] Hartmuth C. Kolb,[†] Teruyuki Kondo,[†] Hoi-Lun Kwong,[†] Dominic V. McGrath,[†] A. Erik Rubin,[†] Per-Ola Norrby,[‡] Kevin P. Gable,[‡] and K. Barry Sharpless*[,†]

Contribution from the Department of Chemistry, The Scripps Research Institute, 10550 North Torrey Pines Road, La Jolla, California 92037, Royal Danish School of Pharmacy, Department of Chemistry, Universitetsparken 2, DK-2100 Copenhagen, Denmark, and Department of Chemistry, Oregon State University, Corvallis, Oregon 97331-4003

Received May 2, 1996[®]

Scheme 1

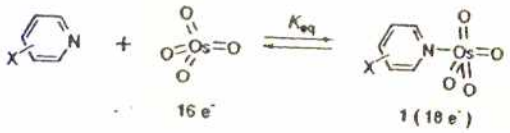

Table 1. Equilibrium Constants for the Binding of Substituted Pyridines to OsO_4 in Organic Solvents (Scheme 1)

pyridine substituent (X)	σ^a	K_{eq} (M^{-1}) acetonitrile	K_{eq} (M^{-1}) toluene
4-N(CH$_3$)$_2$	−0.83	1200 ± 90	1820 ± 230
3,4-(CH$_2$)$_4$	−0.48	143 ± 2	402 ± 100
4-CH$_3$	−0.17	70 ± 3	163 ± 30
none	0.00	34 ± 2	79 ± 7
3-F	0.34	4.1 ± 0.6	17 ± 1
4-CN	0.66	2.0 ± 1.0	4.4 ± 0.8
3,5-(Cl)$_2$	0.74[b]		2.0 ± 1.4

[a] The σ_m parameter was used for substituents at C(3), and the σ_p parameter was used for substituents at C(4). [b] This substituent parameter was obtained by adding the individual σ_m values for both substituents.[27]

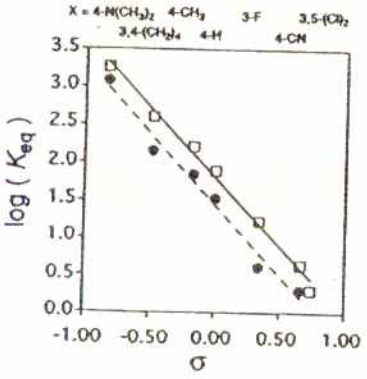

Figure 2. Hammett plots based on the equilibrium constants for the binding of substituted pyridines to OsO_4 in acetonitrile (-●-: $\rho = -1.8$, $r = 0.996$) and toluene (-□-: $\rho = -1.9$, $r = 0.991$) at 25.0 °C.

Scheme 3

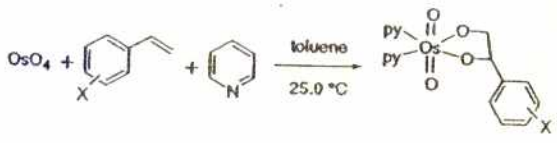

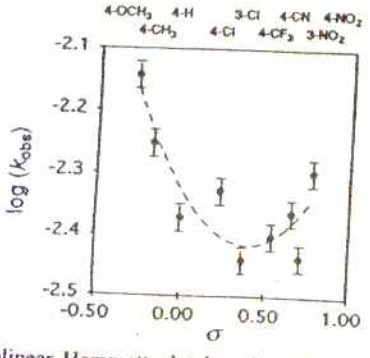

gure 6. Nonlinear Hammett plot based on the pseudo-first-order te constants of Scheme 3 ($[OsO_4]_o = 2.00 \times 10^{-4}$ M, [styrene]$_o$ = 00×10^{-3} M, [py]$_o = 1.25 \times 10^{-1}$ M).

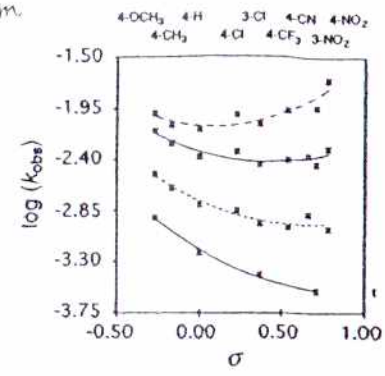

Figure 7. Combined Hammett plots based on the measured pseudo-first-order rate constants for osmylations of substituted styrenes (● = 4-pyrrolidinopyridine, ○ = pyridine, ◆ = 4-cyanopyridine, ◇ = 3,5-dichloropyridine; $[OsO_4]_o = 2.00 \times 10^{-4}$ M, [styrene]$_o = 4.00 \times 10^{-3}$ M, [pyridine]$_o = 1.25 \times 10^{-1}$ M).

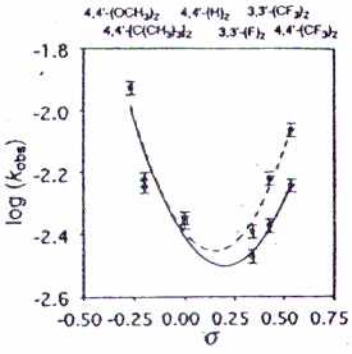

Figure 14. Hammett plots based on the pseudo-first-order rate constants of the DMAP-accelerated osmylations of *trans*-stilbenes in toluene at 25.0 °C ($[OsO_4]_o = 2.00 \times 10^{-4}$ M, [stilbene]$_o = 4.0 \times 10^{-3}$ M; [DMAP]$_o = 1.25 \times 10^{-1}$ M, -●- or 2.5×10^{-2} M, -O-).

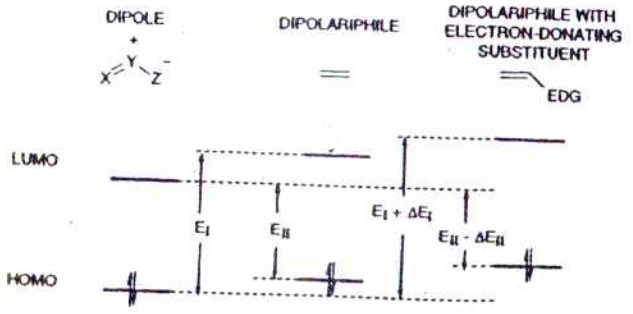

example of Type IV

$$\Delta E_{frontier} = \frac{1}{E_I} + \frac{1}{E_{II}} \quad (5)$$

Figure 18. Frontier molecular orbital interactions proposed to dictate the energy of the transition state in 1,3-dipolar cycloadditions.

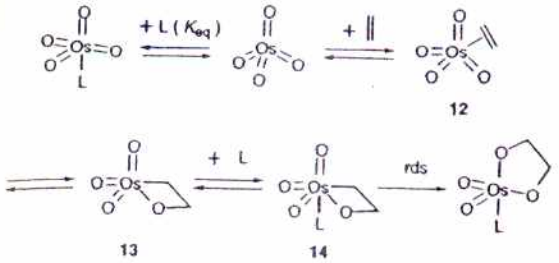

Figure 19. Component equilibria of the proposed stepwise "[2 + 2]" mechanism for the amine-accelerated osmylation of alkenes.

III)-6 Support for [3+2]

<Three case of dipole cycloaddition>

Type I	Type II	Type III
$E_I < E_{II}$	$E_I \doteq E_{II}$	$E_I > E_{II}$

dipole dipolariphile

Condition to accelerate Reaction		Type I	Type II	Type III
	Dipole	EDG	both	EWG
	Dipolariphile	EWG	both	EDG

- From fig 7, 14 stylene and stilben should react with OsO_4 respectively in Type II and Type III.
- IPs of dipolariphiles are directly proportional to the H MO energies.

IPs 8.4eV 7.7eV

- From IPs value, if stylene react with OsO_4 in Type II, stilbene would react in Type I.
⇒ This is inconsistent.

Experimental and Theoretical Kinetic Isotope Effects for Asymmetric Dihydroxylation. Evidence Supporting a Rate-Limiting "(3 + 2)" Cycloaddition

Albert J. DelMonte,[1a] Jan Haller,[1b] K. N. Houk,*[1b] K. Barry Sharpless,*[1c] Daniel A. Singleton,*[1a] Thomas Strassner,[1b] and Allen A. Thomas[1c]

Department of Chemistry, Texas A&M University College Station, Texas 77843
Department of Chemistry, The Scripps Research Institute La Jolla, California 92037
Department of Chemistry and Biochemistry University of California Los Angeles, California 90095-1569

Received May 21, 1997

Table 1. Calculated and Experimental KIEs for Dihydroxylations (3 °C)

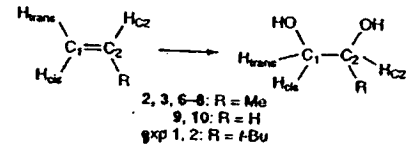

	H_{C2}	H_{cis}	H_{trans}	C_2	C_1
			Calculated[a]		
			(a) "(3 + 2)"		
2	0.907	0.913	0.921	1.025	1.025
3	0.909	0.912	0.921	1.025	1.024
			(b) Formation of an Osmaoxetane		
6	0.892	0.957	0.972	1.050	1.026
7	0.885	0.962	0.980	1.051	1.025
8	0.832	0.927	0.937	1.046	1.021
			(c) Ring-Expansion		
9	0.880	0.964	1.094	0.989	1.039
10	0.933	0.976	1.068	0.984	1.047
			Experiment[b]		
1	0.906(9)	0.919(5)	0.925(7)	1.027(1)	1.028(3)
2	0.908(4)	0.917(8)	0.926(14)	1.026(3)	1.025(3)

[a] See ref 17. [b] Experiments 1 and 2 are reactions carried to 90.5% and 85.6% completion, respectively. Standard deviations are shown in parentheses.

Chart 1 Calculated by Becke3LYP

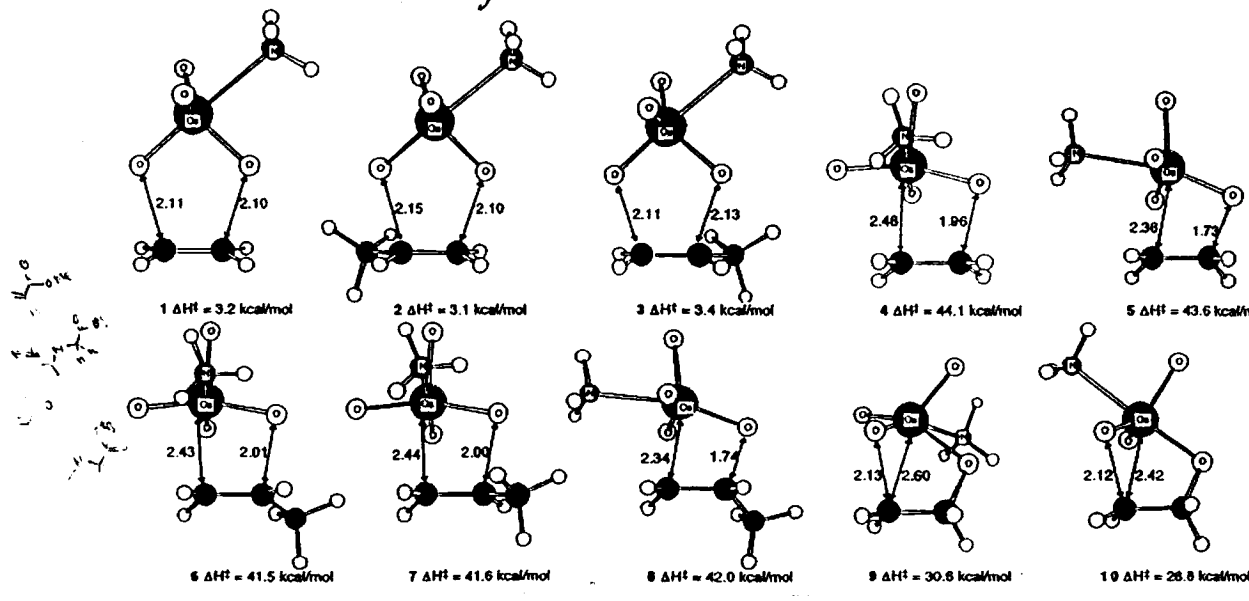

Eth : 1,4,5,9.

: 2,3,6,7,8,10

[3+2] : 1-3

[2+2] : 4-10

* After that, some reports support for [3+2] using computational science.